Eur. Phys. J. A **25**, 107–114 (2005)
DOI 10.1140/epja/i2005-10033-3

THE EUROPEAN PHYSICAL JOURNAL A

The kappa in $J/\Psi \to K^+\pi^-K^-\pi^+$

D.V. Bugg[a]

Queen Mary, University of London, London E1 4NS, UK

Received: 7 April 2005 /
Published online: 24 May 2005 –
Communicated by V.V. Anisovich

Abstract. BES II data for $J/\Psi \to K^*(890)K\pi$ reveal a strong κ peak in the $K\pi$ S-wave near threshold. Both magnitude and phase are determined in slices of $K\pi$ mass by interferences with strong $K_0(1430)$, $K_1(1270)$ and $K_1(1400)$ signals. The phase variation with mass agrees within errors with LASS data for $K\pi$ elastic scattering. A combined fit is presented to both BES and LASS data. The fit uses a Breit-Wigner amplitude with an s-dependent width containing an Adler zero. The κ pole is at $(760 \pm 20(\text{stat}) \pm 40(\text{syst})) - i(420 \pm 45(\text{stat}) \pm 60(\text{syst}))$ MeV. The S-wave $I = 0$ scattering length $a_0 = 0.23 \pm 0.04\ m_\pi^{-1}$ is close to the prediction $0.19 \pm 0.02\ m_\pi^{-1}$ of Chiral Perturbation Theory at $O(p^4)$.

PACS. 13.25.Gv Decays of J/ψ, Υ, and other quarkonia – 14.40.Gx Mesons with $S = C = B = 0$, mass > 2.5 GeV (including quarkonia)

1 Introduction

A possible κ pole at low $K\pi$ mass is controversial. Interest has been aroused by E791 data on $D^+ \to K^-\pi^+\pi^+$ [1], where there is evidence for a scalar resonance of mass $M = 797 \pm 19 \pm 43$ MeV, width $\Gamma = 410 \pm 43 \pm 87$ MeV. However, CLEO, with slightly lower statistics for $D^0 \to K^-\pi^+\pi^0$, find no evidence for the κ [2]. FOCUS data on $D^+ \to K^-\pi^+\mu^+\nu$ require $\bar{K}^{*0}$ interference with either a broad spin zero resonance or a constant amplitude [3].

Wu has presented one solution for the κ from the BES data discussed here [4]. Komada has presented a similar solution [5]. Both these analyses fit the $K\pi$ S-wave using a conventional Breit-Wigner resonance plus a background but do not describe this background. Here a parametrisation based on Chiral Perturbation Theory (ChPT) is used to fit the same data. The Adler zero of ChPT leads to a strongly s-dependent width, which is fitted to the data and replaces the background of refs. [4] and [5]. This fit has the merit of also providing a good fit to LASS data on $K\pi$ elastic scattering [6]. Oller has shown [7] that the E791 data of ref. [1] may also be fitted in a similar fashion consistently with LASS data.

Theoretical opinion on the nature of the κ is divided. Scadron [8] argued in favour of an $SU(3)$ nonet made up of σ, $\kappa(800)$, $f_0(980)$ and $a_0(980)$. The Jülich group of Lohse *et al.* [9] fitted LASS data with t-channel exchanges, but without requiring any κ pole. Further fits to LASS data by Oller *et al.*, based on a unitarisation of chiral perturbation theory, find a κ pole at $M = 770 - i341$ MeV in ref. [10] and at $708 - i305$ MeV in ref. [11]; a later paper of Peláez and Gómez Nicola quotes $(754 \pm 22) - i(230 \pm 27)$ MeV [12]. Schechter *et al.* [13] also argue in favour of a scalar nonet made of σ, κ, $f_0(980)$ and $a_0(980)$. Van Beveren and Rupp have fitted the $K\pi$ S-wave and conclude there is a κ pole at $714 - i228$ MeV [14]. However, Cherry and Pennington [15] assert from LASS data that "There is no $\kappa(900)$", though "data do not rule out a very low-mass κ below 825 MeV". In view of the variety of conclusions, guidance from experiment is obviously needed.

2 Experimental details and data selection

The data selection is conventional and will be outlined only briefly. The data are from 58M J/Ψ hadronic decays in the upgraded BES II detector [16,17]. Charged particles are detected in a vertex chamber and the Main Drift Chamber; these lie inside a solenoidal magnet providing a uniform field of 0.5T. A shower counter is used here purely as a veto for photons; it is made of 12 radiation lengths of lead sheets, interleaved with streamer chambers. Kaons, pions and protons are identified up to 700 MeV/c by a time-of-flight (TOF) array immediately outside the Main Drift Chamber. The σ of the TOF measurement is 180 ps. Further separation is obtained using $\mathrm{d}E/\mathrm{d}x$ in the Main Drift Chamber. The vertex is required to lie within 2 cm of the beam axis and within 20 cm of the centre of the interaction region. All particles are required to lie well within the acceptance of the detector, with charged tracks having polar angles θ of $|\cos\theta| < 0.80$.

[a] e-mail: D.Bugg@rl.ac.uk

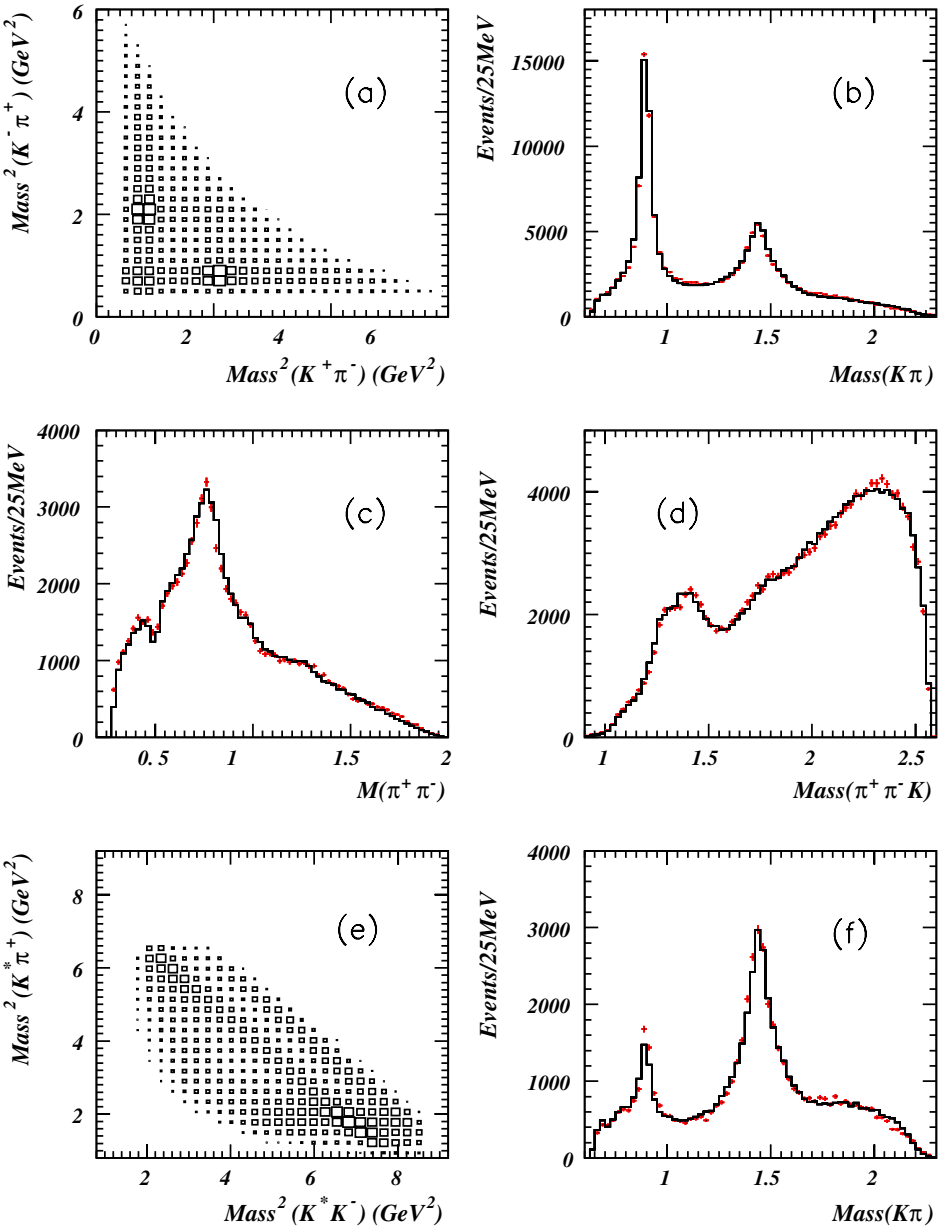

Fig. 1. (a) The scatter plot of $M(K^+\pi^-)$ against $M(K^-\pi^+)$. (b) Projection on to $K^\pm\pi^\mp$ mass; the histogram shows the fit. (c) and (d) Projections on to $\pi\pi$ and $K\pi\pi$ mass. (e) The Dalitz plot for events where one $K^\pm\pi^\mp$ combination is in the mass range 892 ± 100 MeV. (f) Mass projection of the second $K^\mp\pi^\pm$ pair for the same selection as (e).

The slowest two particles always have total energies < 800 MeV. For such energies, kaons and pions differ in momentum by at least 15%. The kinematic separation between K and π in a fit to $K^+\pi^-K^-\pi^+$ is excellent. In addition, both TOF and $\mathrm{d}E/\mathrm{d}x$ are used to calculate χ^2 probabilities for kaons or pions. Monte Carlo studies show that the highest combined probability selects the correct $K^+\pi^-K^-\pi^+$ combination for almost all events, using a cut at $\chi^2 = 40$. An overall probability is required for $K^+K^-\pi^+\pi^-$ higher than for $\pi^+\pi^-\pi^+\pi^-$ or $K^+K^-K^+K^-$ or $K^\pm\pi^\mp\pi^+\pi^-$. Any $K\pi\pi\pi$ combination with $M(\pi^+\pi^-)$ in the interval 497 ± 25 MeV is rejected if $r_{xy} > 8$ mm, where r_{xy} is the distance from the beam axis to the $\pi^+\pi^-$ vertex. This procedure avoids producing a deep cut in genuine $K^+K^-\pi^+\pi^-$ events near the K^0 mass in $\pi^+\pi^-$. The Monte Carlo simulation estimates 215 background events from this source, widely dispersed in $K\pi$ mass. Background from $\phi(1020)\pi^+\pi^-$ is eliminated for $|M(K^+K^-) - M(\phi)| < 20$ MeV. Eventually, there are 77925 selected events. The final-state $K^+\pi^-K^-\pi^+$ has a large branching fraction $\sim 7\times10^{-3}$. Small surviving backgrounds arise from many channels with an extra photon or π^0; Monte Carlo simulations estimate a surviving background of 3.2%, which is fitted as $KK\pi\pi$ phase space.

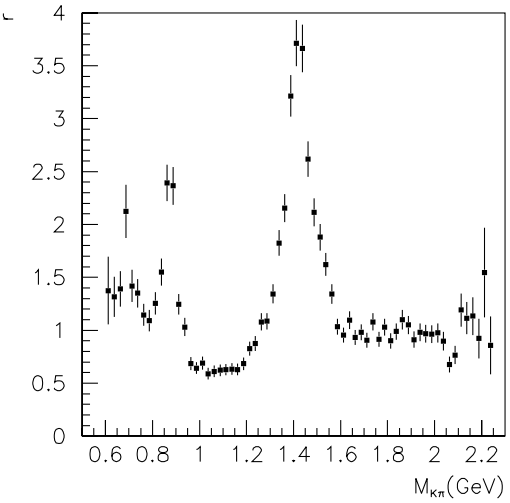

Fig. 2. The $K\pi$ mass projection of fig. 1(f) divided by $K\pi$ phase space, in bins of 20 MeV.

Table 1. Percentage of events fitted to every channel.

Channel	Percentage of events
$K^*(890)K_0(1430)$	30.7 ± 3.5
$K^*(890)\kappa$	18.8 ± 1.5
$K^*(890)K_0(1950)$	2.8 ± 0.6
$K^*(890)K_2(1430)$	7.6 ± 0.5
$K_0(1430)\kappa$	6.8 ± 1.8
$K_0(1430)K_0(1430)$	4.6 ± 0.7
$K_2(1430)K_0(1430)$	2.2 ± 0.2
$K_1(1400)K$	7.9 ± 0.6
$K_1(1270)K$	12.3 ± 1.1
$K_2(1750)K$	1.0 ± 0.3
$a_0(980)\rho(770)$	1.6 ± 0.5
$a_2(1320)\rho(770)$	1.1 ± 0.5
$a_2(1700)\rho(770)$	3.3 ± 0.9
$a_2(1990)\rho(770)$	1.9 ± 0.6
$a_2(2270)\rho(770)$	3.4 ± 0.3
$\phi(1680)f_2(1270)$	1.3 ± 0.4
$\phi(1680)f_0(980)$	0.8 ± 0.2

3 Features of the data

Figure 1(a) shows the scatter plot of $(K^+\pi^-)(K^-\pi^+)$ combinations. There are obvious bands due to $K^*(890)$ and around 1430 MeV, where there are three known K^* resonances. Figure 1(b) shows corresponding peaks in the $K\pi$ mass projection and histograms show the fit described below. Most of the peak at 1430 MeV is fitted as $K_0(1430)$, with only a small contribution from $K_2(1430)$. The $\rho(770)$ is visible in (c). In (d) a strong peak appears due to overlapping $K_1(1270)$ and $K_1(1400)$; there is also a weak $K_2(1770)$ peak.

Evidence for the κ appears in the channel $J/\Psi \to K^*(890)\kappa$, $\kappa \to (K\pi)_S$, where S denotes the S-wave. To illustrate this, one $K^\pm\pi^\mp$ pair (say particles 1 and 2) is selected in the mass range 892 ± 100 MeV. Then fig. 1(f) shows the mass projection of the other $K^\mp\pi^\pm$ pair (particles 3 and 4). Peaks due to $K^*(890)$ and $K_0(1430)/K_2(1430)$ are visible, but there is also a broad $K\pi$ enhancement under the narrow $K^*(890)$. Figure 1(e) shows the Dalitz plot of $K^*K\pi$ combinations with this data selection.

Figure 2 shows the low-mass κ peak more clearly by dividing the $K\pi$ mass projection of fig. 1(f) by $K\pi$ phase space. A definite peak becomes visible in the mass range from threshold to ~ 750 MeV. Analysis given below shows that the κ peak is quite broad, so one should ignore the statistical fluctuation in the bin at 710 MeV.

The $K^*(890)$ peak in fig. 2 does not originate from K^*K^*, which makes a negligible contribution. Instead it originates as follows. Underneath the $K^*(890)$ signal of fig. 1(b) is some κ signal, which is selected by the cut of ± 100 MeV around the $K^*(890)$; these κ events are accompanied by K^* which create the narrow 890 MeV peak in fig. 2. This is the charge conjugate process. Both combinations are included coherently into the amplitude analysis.

In fig. 1(e), the strong diagonal band across the centre of the Dalitz plot is due mostly to $K_0(1430)$. The weaker diagonal band at the upper right-hand edge has a broad component due to the κ and also a narrow component from surviving $K^*(890)$. The horizontal band at the bottom of the plot is due to $K_1(1270)$ and $K_1(1400) \to K^*(890)\pi$.

Across fig. 1(e), there is a substantial ($\sim 15\%$) physics background arising from $a_2\rho$, $a_0\rho$ and $K_1 \to K\rho$; the total ρ contribution is tightly controlled by fitting the magnitude of the ρ peak in fig. 1(c). These channels produce the rather uniform background visible across the scatter plot of fig. 1(a).

4 Amplitude analysis

The amplitude analysis fits events over all of 4-body phase space to channels listed in table 1. This fit follows the standard isobar model, where each amplitude is assigned a complex coupling constant. Data are fitted by the maximum likelihood method to relativistic tensor amplitudes of ref. [18], using 600k Monte Carlo events. Angular momenta L up to 2 in the production process are needed. Standard Blatt-Weisskopf centrifugal barrier factors given in ref. [18] are included using a radius of interaction of 0.8 fm, though results are insensitive to this value.

Table 1 shows the fraction of events fitted to each channel, omitting interferences between channels, but keeping those between different L values within one channel; percentages of events do not add up to exactly 100% because of these interferences. Any amplitude which improves log likelihood by < 30 is omitted; this eliminates possible channels contributing $< 1\%$ of events, *e.g.* unknown K^* above 2 GeV. The dominant channels are $K^*(890)K_0(1430)$, $K^*(890)\kappa$, $K_1(1270)K$ and $K_1(1400)K$; all other channels have little overlap with the essential $K^*(890)\kappa$ signal and very little influence on parameters fitted to the κ. Most resonances are fitted with masses and widths of the Particle Data Group [19]. However, $K_1(1270)$ optimises at $M = 1248 \pm 15$ MeV,

$\Gamma = 157 \pm 35$ MeV, rather wider than the PDG value $\Gamma = 90 \pm 20$ MeV. If PDG values are used instead, parameters for the κ change little, but the overall log likelihood of the fit gets worse.

There is a large $K_0(1430)$ signal in the $K\pi$ S-wave as well as the κ. It interferes strongly with the κ, and it is important to separate $K_0(1430)$ from $K_2(1430)$ and possible $K^*(1410)$ ($J^P = 1^-$). A vital technical feature of the analysis is that decays of the $K^*(890)$ are fitted; that was not done in refs. [4] and [5]. Angular correlations involve 5 angles between i) the $K^*(890)$ decay, ii) the production angle for the $K^*(890)$ and iii) decays of components of the 1430 MeV peak; these correlations provide a secure separation of different J^P, and demonstrate that most of the 1430 MeV peak is due to $[K^*(890)K_0(1430)]_{L=0}$. There is no evidence for any significant $K^*(1410)$. If fitted freely, it contributes only 0.1% of all events. This is not surprising, in view of its $(6.6 \pm 1.3)\%$ branching ratio to $K\pi$ [19].

It is important to ensure that the κ is not a "reflection" due to decays of $K_1(1400)$ and $K_1(1270)$; both populate the low-mass $K\pi$ region. This possibility is eliminated by fitting $K_1(1270)$, $K_1(1400)$ and $K_2(1770)$ to the peaks in fig. 1(d); D- and S-wave decays of both K_1 are included. If the κ signal were a "reflection" from these sources, there would be little change to the fit if the κ is omitted. In fact log likelihood changes by > 1000, a very large amount. A further detail is that $K^*(1400)(J^P = 1^-) \to K^*(890)\pi$ has been tried in the fit. A free fit contributes $< 0.8\%$ of all events, and falls below the cut-off for significant contributions to log likelihood.

4.1 Formulae

The motivation for the formula used to fit the κ will now be discussed. The essential point is to account for the peak in BES data and its absence in elastic scattering. This difference originates from the Adler zero in elastic scattering, which largely cancels the pole. If strong interactions are chirally symmetric, massless pions of zero momentum have zero scattering amplitude. Breaking of chiral symmetry gives the pion a non-zero mass and Weinberg [20] proposed that "soft" pions of low momentum p have a matrix element approximately linear in p^2 and m_π^2. There is then a zero in the scattering amplitude for real pions at $s \simeq m_K^2 - 0.5m_\pi^2$; this Adler zero is a central feature of Chiral Perturbation Theory. It is included here explicitly into an s-dependent width $\Gamma(s)$ for the kappa.

The elastic-scattering amplitude is written as [21]

$$f_{\rm el} = \frac{M_1\Gamma(s)}{M_1^2 - s - iM_1\Gamma(s)}\,, \tag{1}$$

$$\Gamma = \Gamma_0(s - s_A)\exp(-\alpha\sqrt{s})\rho(s), \tag{2}$$

where $\rho(s)$ is the $K\pi$ phase space $2k/\sqrt{s}$, and k is the momentum in the $K\pi$ rest frame; Γ_0 and α are constants. This is the simplest realistic formula containing the Adler zero. In the production process, pions are "hard" because of the large momentum transfer between J/Ψ and the final state. BES data are then fitted with a complex coupling constant $G_{J/\Psi}$:

$$f_{\rm prod} = \frac{G_{J/\Psi}}{M_1^2 - s - iM_1\Gamma(s)}. \tag{3}$$

Since the Adler zero is a feature of the full $K\pi$ S-wave amplitude, the $K_0(1430)$ is fitted with the Flatté formula

$$\Gamma(s) = \frac{s - s_A}{M_2 - s_A}[g_1\rho_{K\pi}(s) + g_2\rho_{K\eta'}(s)]; \tag{4}$$

however, the Adler zero plays only a small role for $K_0(1430)$ in practice.

For elastic scattering, unitarity is satisfied by adding the phases of $K_0(1430)$ and κ; this is the Dalitz-Tuan prescription [22]. For J/Ψ decays there are hundreds of open channels, so unitarity no longer makes any effective constraint; in this case, the standard procedure of adding the amplitudes is used. Note that it is being assumed that the κ peak may be fitted as a resonance, *i.e.* a pole. If there were a substantial non-resonant background, this would not be true. At the end of the analysis, the possible requirement for background will be examined, but no significant evidence for such a background emerges. The stability of the κ pole will be examined by trying a variety of other assumptions for the s-dependence of both resonances.

Parameters of $K_0(1430)$ are constrained to fit the peaks in both BES and LASS data [6]: BES data determine the mass and width best, but LASS data determine better the ratio g_2/g_1. Parameters for the $K_0(1430)$ optimise at $M_2 = 1.535 \pm 15(\text{stat}) \pm 10(\text{syst})$ GeV, $g_1 = 0.361 \pm 15 \pm 20$ GeV, $g_2/g_1 = 1.0^{+0.3}_{-0.2}$. The pole lies at $M_2 = (1433 \pm 30 \pm 10) - i(181 \pm 10 \pm 12)$ MeV. Note that the full width of a conventional Breit-Wigner resonance is twice the imaginary part of M_2; the width quoted by the PDG is 294 ± 23 MeV.

The κ line-shape is highly distorted in elastic scattering by the Adler zero. The phase shift must follow the unitarity relation $f_{\rm el} = \sin\delta e^{i\delta}/k$ up to the inelastic threshold. The phase shift required by LASS data rises slowly from threshold and passes 90° only close to $K_0(1430)$. This requires a value of M_1 in eq. (1) well above 1430 MeV, despite the pole near threshold. This unusual feature is discussed by Zheng *et al.* [23], who propose an s-dependent width similar to that adopted here. The value of M_1 may be fitted anywhere in the range 2.4 to 4.0 GeV if Γ_0 is re-optimised. The fit given here uses $M_1 = 3.3$ GeV, $\Gamma_0 = 24.53$ GeV, $\alpha = 0.4$ GeV^{-1}, though these are highly correlated. Extrapolating the amplitude off the real s-axis, the pole is at $M_1 = (760 \pm 20(\text{stat}) \pm 40(\text{syst})) - i(420 \pm 45(\text{stat}) \pm 60(\text{syst}))$ MeV. The corresponding full-width is large: 840 MeV; systematic errors will be discussed below. The width is much larger than the value $410 \pm 43 \pm 87$ MeV found by E791 [1]; they did not include the Adler zero, but they did include an interfering flat background over the Dalitz plot.

Removing $K^*(890)\kappa$ gives the fit shown by the histogram of fig. 3(a); this is obviously unsatisfactory. Using the scattering length formula of LASS gives a very similar fit, because there is no κ peak at low mass. For the

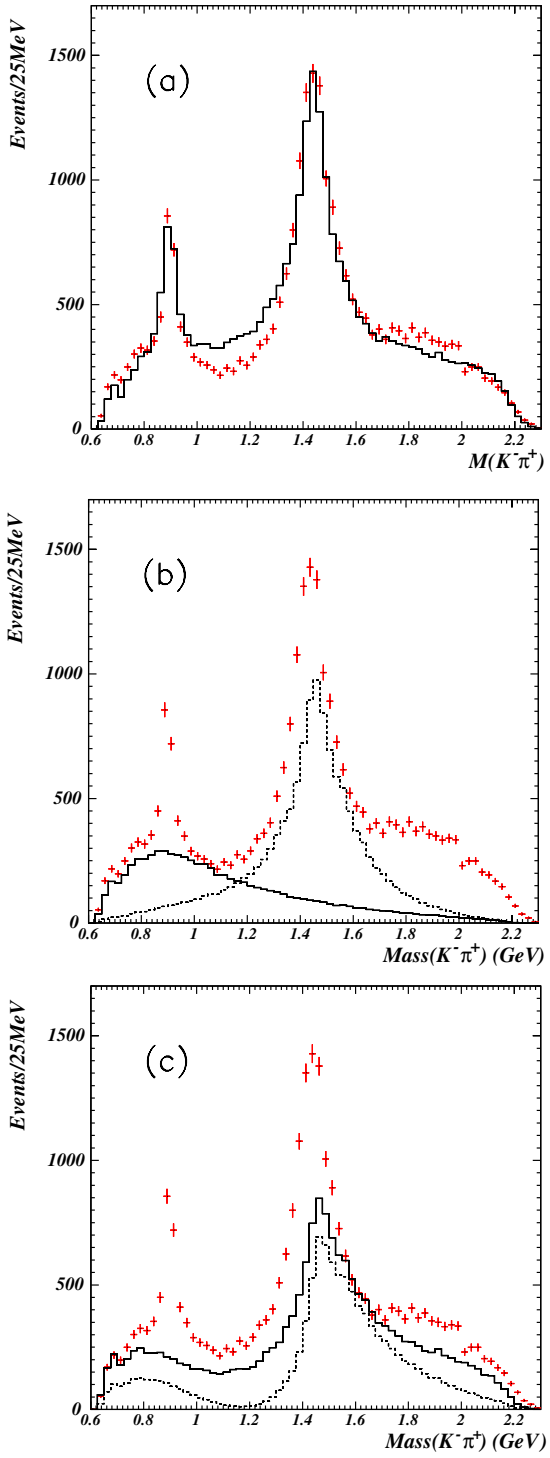

Fig. 3. (a) The poor fit when the channel $K^*(890)\kappa$ is removed; (b) individual contributions from κ (full histogram) and $K_0(1430)$ (dashed histogram); (c) the coherent sum of κ + $K_0(1430)$ (dashed histogram) and the coherent sum κ + $K_0(1430)$ + $K_1(1270)$ + $K_1(1400)$ (full histogram).

final fit, figs. 3(b) and (c) show contributions to the $K\pi$ mass projection with the data selection of figs. 1(e) and (f). Figure 3(b) shows intensities of κ (full histogram) and $K_0(1430)$ (dashed histogram). In fig. 3(c), the dashed histogram shows the coherent sum of κ and $K_0(1430)$; there is strong destructive interference between them, simulating a low-mass peak of width $\sim$ 400 MeV. The full histogram of fig. 3(c) shows the coherent sum of κ, $K_0(1430)$, $K_1(1270)$ and $K_1(1400)$. The difference between data and the full histogram arises from i) further contributions from $K^0(1430)K^0(1430)$ and $K^0(1430)\kappa$, ii) interferences with other components, mostly K_1K with $K_1 \to K\rho$.

4.2 The width of the κ

In view of the width of the low-mass κ peak $\sim$ 400 MeV and the similar width fitted by E791, an attempt has been made to force the global fit to this width. It produces a distinctly different solution with large changes in the phases fitted to $K_1(1270)$, $K_1(1400)$ and $K_0(1430)$. Such a solution is metastable over a limited range of parameters. However, it readily collapses to the fit reported here, with an improvement in log likelihood of $\sim$ 10 standard deviations. Attempts to fit LASS data with this width also fail to give an acceptable fit unless additional s-dependence is added to the width; that leads to instablility in the mass range from the $K\pi$ threshold to 825 MeV, where the LASS data begin. If the scattering length is then fixed to the prediction of Chiral Perturbation Theory, a width of at least 630 MeV is required.

5 The phase of the κ

The phase variation of the κ with mass will now be discussed. It is well determined by BES data by two major interferences: a) with the channel $K_0(1430)K^*(890)$, b) with $K_1(1270)K$ and $K_1(1400)K$.

As a direct check that data are consistent with the phase variation of eq. (3), the $\kappa \to K\pi$ contribution to BES data may be fitted in slices of $K\pi$ mass up to 1700 MeV; above that the κ amplitude becomes too small to be determined reliably because of uncertainty in $K_0(1950)$. Four alternatives slice fits have been examined. In the most restrictive, the phase is fitted in one bin at a time, keeping the magnitude fixed to that of the global fit. All other amplitudes are refitted freely in magnitude and phase except one; (one phase must be fixed and the maximum likelihood method depends on one magnitude also being fixed). Convergence is fastest if this is chosen to be the largest amplitude, $[K_0(1430)K^*(890)]_{L=0}$ but alternatives give the same result. In the bin from 1400 to 1500 MeV, the phase cannot be determined accurately because the κ signal is swamped by the large $K_0(1430)$ peak.

Figure 4(a) shows results as points, compared with the global fit (full line). There is no systematic tendency for points to move away from the global fit. Note that in fitting BES data, the $K^*(890)\kappa$ amplitude has an overall phase fitted freely to the isobar model. The curve in fig. 4(a) has been drawn so that the phase goes to zero at the $K\pi$ threshold; therefore, only the phase variation with mass is meaningful. Points

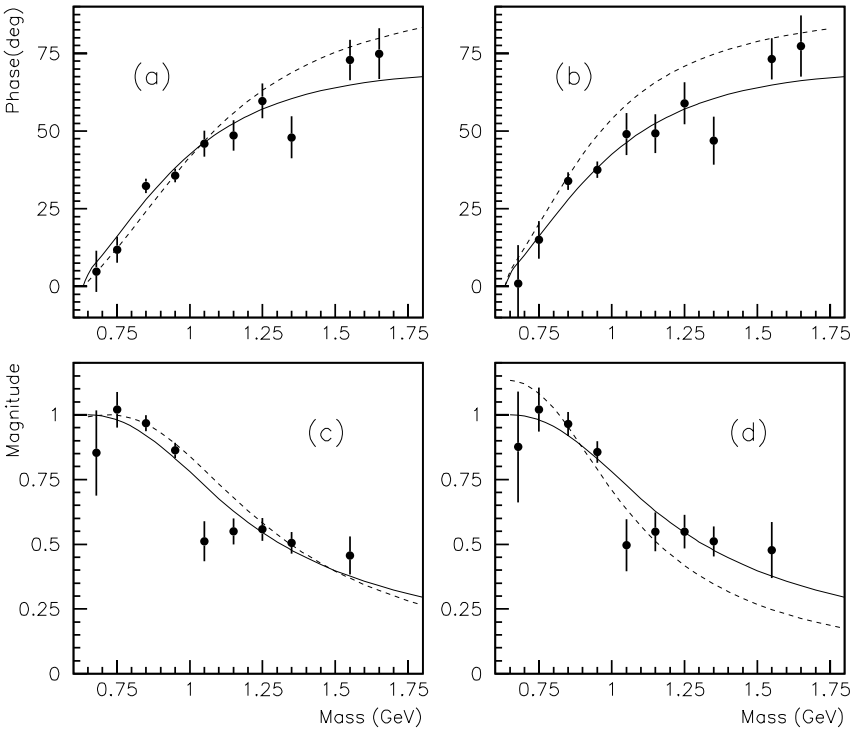

Fig. 4. (a) Points show the phase of the κ amplitude, determined bin by bin; the magnitude is fixed from the global fit. (b) Phases when both magnitudes and phases are fitted in all bins simultaneously. (c) Magnitudes when magnitudes and phases are both fitted bin by bin. (d) Magnitudes when both magnitudes and phases are fitted freely in all bins. Full curves show the global fit. Dashed curves in (a) and (c) show the optimum fit to BES data alone. Dashed curves in (b) and (d) show the fit to BES data with a Breit-Wigner amplitude of constant width.

are determined directly as deviations from the global fit. The phase of the $[K^*(890)\kappa]_{L=0}$ amplitude relative to $[K^*(890)L_0(1430)]_{L=0}$ is $2.28^c \pm 0.02^c$ and for $[K^*(890)\kappa]_{L=2}$ is $4.82^c \pm 0.04^c$. These correspond to the phases of elastic scattering of κ from $K^*(890)$ at the mass of the J/Ψ and can in principle take any values.

The errors will now be discussed. Statistics are very high (79k events) and it is common experience elsewhere that, with these statistics, changes of log likelihood from bin to bin may be above statistics; this can arise from the neglect of small signals below 1% intensity and also from approximations in the Monte Carlo. Here it is found that statistical errors indeed need to be multiplied by a factor 2.1 to allow for this. Errors also include allowance for one standard deviation changes in masses and widths of all resonances; the main systematic error arises from parameters of $K_0(1430)$.

Next, the phase is fitted in all bins simultaneously, but fixing the magnitude to the global fit. Results are not shown because they are almost identical to fig. 4(a). The reason is that separate bins contain different events. The only correlation between bins arises from interference with $K_1(1270)$ and $K_1(1400)$; one bin can pull the phase of K_1 amplitudes slightly, and this reacts on other bins. However, correlations between bins are only $\sim 5\%$.

Finally, magnitude and phase are set free in all bins simultaneously. It is however, necessary to fix the κ amplitude in the bin from 1400 to 1500 MeV and above 1700 MeV; the intensity in these bins is only 10% of the integrated κ intensity. Results are shown in fig. 4(b). There is no essential change from fig. 4(a) but errors increase because of statistical fluctuations in the magnitude; this correlates with the fitted phase, because the intensity in each bin depends on the real part of interferences, *i.e.* on both magnitude and phase.

Figure 4(c) shows the magnitude fitted in one bin at a time if both magnitude and phase are set free together. Figure 4(d) shows the worst case, where magnitude and phase are set free in all bins simultaneously; there is little difference from fig. 4(c). Note that figs. 4(c) and (d) show magnitudes; intensities are the squares of these and are rather small for masses above 1200 MeV.

The conclusion from figs. 4(a) and (b) is that the phase variation of the κ amplitude from BES data is the same as the phase variation for elastic scattering within errors. This is not a surprising result. It is well known that the partial-wave amplitude can be written in the form $f(s) = N(s)/D(s)$ [24]. Here the numerator $N(s)$ is real and arises from the left-hand cut, *i.e.* from driving forces. The denominator $D(s)$ is complex and arises from the right-hand cut, *i.e.* $K\pi$ rescattering. The pole terms in $D(s)$ are common to all channels coupled to $K\pi$. What the data tell us is that a single κ pole term plus $K_0(1430)$ fits the data up to ~ 1700 MeV. This hypothesis can be tested directly by adding a further pole. The LASS data rule out the possibility of a pole below 1950 MeV. Any further pole above that mass improves log likelihood for BES data by less than three standard deviations.

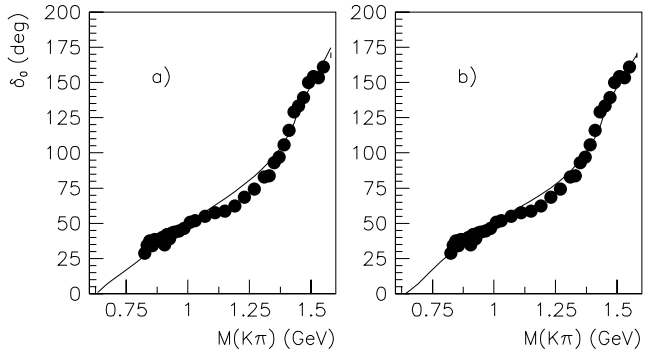

Fig. 5. (a) Optimum fit to LASS data from eqs. (1)-(4). (b) Improved fit allowing one extra parameter in fitting LASS data.

The main sources of systematic error in this result lie at masses above 1200 MeV. They arise from i) uncertainty in the precise line-shape for $K_0(1430)$ and ii) cross-talk with the small $K_0(1950)$ signal. Figure 5(a) shows the fit to LASS data. There is a small systematic discrepancy in the mass range around 1250 MeV. It is of similar magnitude to discrepancies between Estabrooks *et al.* [25] and Aston *et al.* [6]. It can be reduced in several alternative ways. One is to add a further factor $(1+\beta s)$ to the phase of the κ amplitude; the result is shown in fig. 5(b). The κ pole moves to $697 - i336$ MeV. An alternative is to allow some further inelasticity into $K_0(1430)$, due to decays to $K^*\rho$ or $\kappa\sigma$; the LASS group quotes a $\pm 9\%$ normalisation uncertainty which allows a modest amount of such inelasticity. A similar effect may be obtained by allowing some inelasticity into the κ amplitude; π exchange between K and π allows production of the final-state $\kappa\sigma$. A calculation of the magnitude of such an effect would be valuable along the lines suggested by Wu and Zou [26].

Returning to figs. 4(a) and (c), the dashed lines show the optimum fit to the κ for BES data alone. This requires $\alpha = 0$ in the exponential of eq. (2). The fit to BES data improves by 3.8 standard deviations; the κ becomes narrower, with a pole position of $753 - i319$ MeV. However, the price is that the $K_0(1430)$ required to fit LASS data is then definitely wider than that required by BES data. This inconsistency suggests it is not a real physical effect.

The FOCUS Collaboration has recently measured the phase of the $K\pi$ S-wave amplitude in D^+ decays to $K^-\pi^+\mu^+\nu$ [27]. The μ and ν are weakly interacting, so Watson's theorem applies rigorously. They find a phase for the $K\pi$ S-wave in excellent agreement with LASS data. So BES, FOCUS and LASS data agree on the phase of the $K\pi$ S-wave, and hence with the N/D formalism. However, FOCUS find a phase in strong disagreement with the phase of the κ amplitude used by E791 for the similar process $D^+ \to K^-\pi^+\pi^+$. The κ amplitude needed by E791 is small; it is important to check whether it can be fitted by the LASS effective range formulae; if so, that would resolve the discrepancy.

A final comment is that the phase of the κ amplitude could be affected by rescattering of its decay products from the spectator pion. Such so-called triangle diagrams have been discussed by Anisovich and Ansel'm [28]. This rescattering is what generates the phase of the coupling constant appearing in the isobar model. It could in principle vary over the mass range of the κ. The present analysis does not call for such an effect beyond the combined experimental errors of BES and LASS data. Another possible rescattering effect amongst final-state particles is the appearance of a t-channel pole in $K\pi$ due to exchange of $K^*(890)$ or $\rho(770)$; however, such exchanges are the driving forces which are conventionally believed to drive $K\pi$ elastic scattering and hence the κ pole.

6 Alternative fits

A second test has been made using for the κ a Breit-Wigner amplitude of constant width, *i.e.* no $\rho(s)$ factor in $\Gamma(s)$. The best fit is shown by the dashed curves in figs. 4(b) and (d). This fit requires $M_1 = 718$ MeV, $\Gamma = 1045$ MeV, corresponding to a pole position of $M_1 = 844 - i444$ MeV. The phase variation with mass is close to that of elastic data. However, it requires a phase shift of 81° at threshold in elastic scattering, and this is clearly unphysical.

A fit to the κ using $\Gamma = \Gamma_0\rho(s)$ gives a very bad fit, worse than eqs. (1)-(3) by > 15 standard deviations. It requires $M_1 = 1035$ MeV, $\Gamma_0 = 725$ MeV, and a pole position of $1043 - i410$ MeV. The problem is that it requires a phase variation of 90° between threshold and the resonance mass; both BES and LASS data disagree strongly with this. However, as the Ishida group has shown [29], the elastic data may be fitted with a conventional Breit-Wigner resonance with $\Gamma(s) \propto \rho(s)$ if one adds a background phase decreasing rapidly with s, and cancelling a large part of the resonant phase shift. Both LASS and BES data can be fitted in this way, but only if the background is the same in both sets of data within the errors. This is algebraically equivalent to including the s-dependence of the background into $\Gamma(s)$. The fit reported by Komada [5] does in fact contain a background, but details of this background are not given. Komada reports a mass of $M = 882 \pm 24$ MeV. This is clearly incompatible with the peak shown here in fig. 2, unless such a background is included and plays a major role.

7 Conclusions

The essential result from this analysis is evidence for a low-mass $K\pi$ S-wave enhancement which definitely peaks close to threshold. Equations (1)-(4) including the Adler zero give a pole at $M = (760 \pm 20(\text{stat}) \pm 40(\text{syst})) - i(420 \pm 45(\text{stat}) \pm 60(\text{syst}))$ MeV. The main systematic uncertainty lies in the width. This is because the fitted magnitude above 1200 MeV is sensitive to the large $K_0(1430)$ signal, hence its precise line-shape. The second result is that the fit reported here achieves consistency with LASS data; the phase variation observed for the κ is consistent with that from elastic scattering. A similar result was obtained earlier for the σ [30].

From the best fit to both LASS and BES data, the $K\pi$ $I = 0$ scattering length is $(0.23 \pm 0.04)m_\pi^{-1}$. This is in close agreement with the prediction of Chiral Perturbation Theory at order p^4, namely $(0.19 \pm 0.02)m_\pi^{-1}$ [31].

I wish to thank the BES Collaboration for the use of the data and the Royal Society for financial support of collaboration between BEPC and Queen Mary, London, contract Q771. I also wish to thank Dr. L.Y. Dong for extensive assistance in processing data and Prof. B.S. Zou for discussions about the physics over a period of many years.

References

1. E791 Collaboration (E.M. Aitala *et al.*), Phys. Rev. Lett. **89**, 21802 (2002).
2. CLEO Collaboration (S. Kopp *et al.*), Phys. Rev. D **63**, 092001 (2001).
3. FOCUS Collaboration (J.M. Link *et al.*), Phys. Lett. B **535**, 43 (2002).
4. BES Collaboration (N. Wu), *International Symposium on Hadron Spectroscopy, Chiral Symmetry and Relativistic Description of Bound Systems, Tokyo, February 24-26, 2003*, KEK report no. 28 (2003) p. 143.
5. BES Collaboration (T. Komada), AIP Conf. Proc. **717**, 337 (2004).
6. LASS Collaboration (D. Aston *et al.*), Nucl. Phys. B **296**, 253 (1988).
7. J.A. Oller, hep-ph/0411105.
8. M.D. Scadron, Phys. Rev. D **26**, 239 (1982).
9. D. Lohse *et al.*, Phys. Lett. B **234**, 235 (199).
10. J.A. Oller, E. Oset, J.R. Peláez, Phys. Rev. D **60**, 074023 (1999).
11. M. Jamin, J.A. Oller, A. Pich, Nucl. Phys. B **587**, 331 (2000).
12. J.R. Peláez, A. Gómez Nicola, Phys. Rev. D **65**, 054009 (2002); AIP Conf. Proc. **660**, 102 (2003).
13. D. Black, A.H. Fariborz, F. Sannino, J. Schechter, Phys. Rev. D **59**, 074026 (1999).
14. E. van Beveren, G. Rupp, Euro. Phys. J. C **22**, 493 (2001).
15. S.N. Cherry, M.R. Pennington, Nucl. Phys. A **688**, 823 (2001).
16. BES Collaboration (J.Z. Bai *et al.*), Nucl. Instrum. Methods A **344**, 319 (1994).
17. BES Collaboration (J.Z. Bai *et al.*), Nucl. Instrum. Methods A **458**, 627 (2001).
18. B.S. Zou, D.V. Bugg, Eur. Phys. J. A **16**, 537 (2003).
19. Particle Data Group (PDG) (S. Eidelmann *et al.*), Phys. Lett. B **592**, 1 (2004).
20. S. Weinberg, Phys. Rev. Lett. **17**, 616 (1966).
21. D.V. Bugg, Phys. Lett. B **572**, 1 (2003).
22. R.H. Dalitz, S. Tuan, Ann. Phys. (N.Y.) **10**, 307 (1960).
23. H.Q. Zheng *et al.*, Nucl. Phys. A **733**, 235 (2004), arXiv: hep-ph/0310293.
24. M. Jacob, F.F. Chew, *Strong Interaction Physics* (Benjamin, New York, 1964) pp. 121-123.
25. P. Estabrooks *et al.*, Nucl. Phys. B **133**, 490 (1978).
26. F.Q. Wu, B.S. Zou, arXiv: hep-ph/0412276.
27. FOCUS Collaboration (J.M. Link *et al.*), hep-ex/0503043.
28. V.V. Anisovich, A.A. Ansel'm, Sov. Phys. Usp. **88**, 117 (1966).
29. S. Ishida *et al.*, Prog. Theor. Phys. **98**, 621 (1997).
30. D.V. Bugg, Eur. Phys. J. C **37**, 433 (2004).
31. V. Bernard, N. Kaiser, U.G. Meissner, Nucl. Phys. B **357**, 129 (1991).